

Starburst-like Dust Extinction in the Small Magellanic Cloud

Karl D. Gordon and Geoffrey C. Clayton

Department of Physics & Astronomy, Louisiana State University

Baton Rouge, LA 70803

email: (gordon,gclayton)@fenway.phys.lsu.edu

ABSTRACT

The recent discovery that the UV dust extinction in starburst galaxies is similar to that found in the Small Magellanic Cloud (SMC) motivated us to re-investigate the ultraviolet (UV) extinction found in the SMC. We have been able to improve significantly on previous studies by carefully choosing pairs of well matched reddened and unreddened stars. In addition, we benefited from the improved S/N of the NEWSIPS *IUE* data and the larger sample of SMC stars now available. Searching the *IUE* Final Archive, we found only four suitable early-type stars that were significantly reddened and had well matched comparison stars. The extinction for three of these stars is remarkably similar. The curves are roughly linear with λ^{-1} and have no measurable 2175 Å bump. The fourth star has an extinction curve with a significant 2175 Å bump and weaker far-UV extinction. The dust along all four sightlines is thought to be local to the SMC. There is no significant Galactic foreground component. The first three stars lie in the SMC Bar and the line-of-sight for each of them passes through regions of recent star formation. The fourth star belongs to the SMC Wing and its line-of-sight passes through a much more quiescent region. Thus, the behavior of the dust extinction in the SMC supports a dependence of dust properties on star formation activity. However, other environmental factors (such as galactic metallicity) must also be important. Dust in the 30 Dor region of the LMC, where much more active star formation is present, does not share the extreme extinction properties seen in SMC dust.

Subject headings: dust, extinction – galaxies: individual (SMC) – galaxies: ISM – galaxies: starburst – ultraviolet: ISM

1. Introduction

The interstellar dust in the Small Magellanic Cloud (SMC) has gained new importance with the discovery that its ultraviolet (UV) extinction is uniquely similar to extinction found in starburst galaxies (Calzetti et al. 1994; Gordon, Calzetti, & Witt 1997). Dust in the Galaxy and the Large Magellanic Cloud does not show starburst galaxy-like extinction. Starburst galaxies are

the only type of galaxy that has been detected from low to high ($z > 2.5$) redshifts (Kinney et al. 1993; Steidel et al. 1996; Lowenthal et al. 1997; Trager et al. 1997; Franx et al. 1997). These galaxies serve as an excellent probe of galaxy evolution through the study of their star formation and metal enrichment rates at different redshifts. The derivation of these rates for high redshift galaxies is sensitive to the adopted UV dust extinction (Pettini et al. 1997; Madau, Pozzetti, & Dickinson 1997). Thus, understanding the physical processes responsible for producing the starburst-like dust seen in the SMC is important to the modeling of starburst galaxies.

In addition, the study of the UV extinction curve in Local Group galaxies promises to help in determining the sizes, shapes, and materials which make up dust grains. Ultraviolet extinction curves have been determined in the Milky Way, the Large Magellanic Cloud (LMC), the SMC, and (tentatively) M31. The extinction curves in these four galaxies paint a complex picture of the environmental dependence of dust properties. In the Milky Way, Cardelli, Clayton, & Mathis (1989, hereafter CCM) found that the infrared to UV extinction curves can be described fairly well by a relationship which depends on only one parameter, $R_V = A_V/E(B - V)$ which is a measure of the overall dust grain size. There are significant deviations from the CCM relation in different Galactic environments (Mathis & Cardelli 1992). In the LMC, the UV extinction curves show a distinctly different behavior between the 30 Dor region (a mini-starburst [Walborn 1991]) and the rest of the LMC (Clayton & Martin 1985; Fitzpatrick 1985, 1986). The 2175 Å bump is weaker and the far-UV rise is stronger in the 30 Dor region than in the rest of the LMC which have strengths similar to the average Galactic extinction curve. In the SMC, the average extinction curve is characterized by a roughly linear rise (versus λ^{-1}) increasing toward shorter wavelengths without a 2175 Å bump (Prévot et al. 1984; Thompson et al. 1988). Yet, there is one sightline which has an extinction curve with a significant 2175 Å bump (Lequeux et al. 1982). In M31, the extinction curve is consistent with that of the average Galactic extinction within the associated uncertainties, although the 2175 Å bump may be weak (Bianchi et al. 1996). The complex behavior in these four galaxies implies that the physical properties of dust grains may be dependent on a multitude of environmental parameters. Two of these are metallicity and star formation activity both of which may affect the overall composition and size distribution of dust grains (Clayton & Martin 1985; Fitzpatrick 1985; CCM; Gordon et al. 1997).

2. Previous Work

There have been a number of papers based in part or entirely on the derivation of SMC UV extinction curves (Lequeux et al. 1982; Prévot et al. 1984; Thompson et al. 1988; Rodrigues et al. 1997). These studies used the pair method to derive extinction curves (see §3.1). The extinction curves were derived by comparing a reddened SMC star to an unreddened SMC star or (more commonly) a group of unreddened SMC stars. Using unreddened stars of the same temperature and luminosity as the reddened stars is crucial to determining accurate extinction curves. All of the previous work suffered from poor spectral matching between reddened and unreddened stars

due in part to the paucity of accurate optical and/or UV 2D spectral types. Recent work has provided 2D spectral types in both the optical (Garmany, Conti, & Massey 1987; Massey et al. 1995; Lennon 1997) and UV (Neubig & Bruhweiler 1997). The previous studies also suffered from low signal-to-noise spectra due to the faintness of the stars in the SMC. The signal-to-noise ratio and absolute calibration of all the spectra taken by the International Ultraviolet Explorer (*IUE*) have been greatly improved through the NEWSIPS reduction routines (Nichols et al. 1994). Also, there is now a larger sample of SMC stars observed with *IUE* than were available a decade or more ago when the previous studies were done. Thus, the UV extinction curves in the SMC can be greatly improved using star pairs that are better spectral matches and have higher S/N spectra. We list the reddened stars used in previous works in Table 1 along with comments on the quality of the derived extinction curves.

Most of the previous work has been done by three groups, one based in France, one in England, and one in Brazil. The final results of the French group are presented in Lequeux et al. (1982) and Prévot et al. (1984) which supersede earlier work (Rocca-Volmerange et al. 1981; Lequeux et al. 1984). In Prévot et al. (1984), this group determined the best (and often used) average UV extinction curve for the SMC from only *three* reddened stars (AZV 18, AZV 398, & SK 191). One drawback to this paper is that the individual extinction curves are not shown, just the average which makes it difficult to assess the accuracy of the individual curves. The star, SK 191, is an essentially unreddened star, making its extinction curve useless. In addition, Prévot et al. (1984) derived extinction curves for two other stars, but excluded them as having “anomalous” extinction curves. These other two stars were AZV 393 (Lequeux et al. 1984) and AZV 456 (Lequeux et al. 1982). AZV 393 is an unreddened star with a UV spectral type of B3 Ia (Neubig & Bruhweiler 1997). The extinction curve for AZV 456 is real and significantly different from the average SMC extinction (Lequeux et al. 1982). This is the only curve in the SMC which shows the presence of the 2175 Å bump. However, the extinction curve, derived by this group for AZV 456, suffers from a spectral mismatch which shows up in an asymmetric 2175 Å bump. This is due to a mismatch between the reddened and comparison stars in the Fe III lines around 2000 Å which are luminosity and temperature sensitive (Cardelli, Sembach, & Mathis 1992; Neubig & Bruhweiler 1997). The validity of the Prévot et al. (1984) average extinction curve is called into question through their inclusion of a highly uncertain extinction curve (SK 191) and their exclusion of the “anomalous” extinction curve of AZV 456.

The final results of the English group are contained in Thompson et al. (1988) which supersedes earlier work (Nandy et al. 1982; Bromage & Nandy 1983). In Thompson et al. (1988) a sample of four reddened stars (AZV 18, 56, 373, & SK 191), when compared to the unreddened star AZV 264, produced a UV extinction curve consistent with the Prévot et al. (1984) average curve. This was done instead of calculating individual extinction curves as all of the reddened stars, except for AZV 18, are only lightly reddened ($\Delta(B - V) < 0.13$) making their extinction curves highly uncertain.

The Brazilian group’s work is presented in Rodrigues et al. (1997). They calculate UV

Table 1. Previous Extinction Work

AZV ^a	SK ^b	ref ^c	quality ^d	comments
18 ^e	13	P84,T88	good	good comparison
20	14	R97	bad	spectral type too late (A0Ia)
56	31	T88	bad	too bright for reddened star
126		R97	bad	unreddened star
211	74	R97	bad	spectral type too late (A0Ia)
373	119	T88	bad	very low $E(B - V)$
398 ^e		P84,R97	good	good comparisons
456 ^e	143	L82,R97	poor	spectral mismatch
	191	P84,T88	bad	unreddened star

^aAzzopardi, Vigneau, & Macquet 1975; Azzopardi & Vigneau 1979; 1982

^bSanduleak 1968, 1969

^cL82 = Lequeux et al. 1982; P84 = Prèvot et al. 1984; T88 = Thompson et al. 1988; R97 = Rodrigues et al. 1997

^dThe quality of the extinction curve was good (reddened star and at least one good comparison star), poor (reddened star and no good comparison stars), or bad (star unsuitable for extinction curve work)

^eUsed in this study

extinction curves for five stars – AZV 20, 126, 211, 398, & 456. Two of these stars, AZV 20 & 211, have A0 Ia spectral types. Stars with spectral types later than about B5 are normally not used for UV extinction work. This is due to their lower UV fluxes and the rapid change in their intrinsic spectra as a function of spectral type (Rodrigues et al. 1997). These problems resulted in extinction curves for these two stars (shown in Fig. 2 of Rodrigues et al. [1997]) which are very noisy (AZV 20) or have odd changes of slope (AZV 211). The extinction curve for AZV 126 presented by Rodrigues et al. (1997) has a very shallow slope which is a result of comparing the unreddened star (AZV 126) to other unreddened stars of earlier spectral types. The UV spectral type of AZV 126 is B1 II and the UV spectral types of the comparison stars, AZV 61, 317, and 454, are O5 III, O7 Ia, and O9 V, respectively (Neubig & Bruhweiler 1997). The extinction curves for AZV 398 and 456 presented by Rodrigues et al. (1997) reproduce the work of Prévot et al. (1984).

From a careful analysis of the previous work on the extinction curves in the SMC, only three reddened stars (AZV 18, 398, & 456) emerge as good candidates for extinction curve work.

3. Extinction Curves

We collected all the stars with spectral types between O9 and B3 in the SMC with *IUE* low dispersion spectra in order to have the largest possible sample of reddened and unreddened stars. Optical and UV spectral types were taken from the literature (Bouchet et al. 1985; Garmany et al. 1987; Massey et al. 1995; Lennon 1997; Neubig & Bruhweiler 1997). From this list, candidate reddened stars were identified as having red ($B - V$) colors when compared to other stars with similar optical and UV spectral types.

For each candidate reddened star, we attempted to identify a comparison star which satisfied the three Fitzpatrick criteria (Fitzpatrick 1985). In addition, we required the $\Delta(B - V)$ between the reddened and comparison star to be greater than 0.15. The first Fitzpatrick criterion requires that $\Delta(U - B)/\Delta(B - V)$ has a value appropriate for reddening due to dust. The average value of $\Delta(U - B)/\Delta(B - V)$ for the SMC is 0.81 ± 0.11 (Bouchet et al. 1985). The second Fitzpatrick criterion requires that ΔV_o , which is the difference between the dereddened V magnitude of the reddened star and the V magnitude of the comparison star, is less than 0.8 magnitudes. This criterion insures the luminosities of the two stars are comparable as all stars in the SMC are located at approximately the same distance. The reddened star's V magnitude was dereddened using $R_V = 2.72$ (Bouchet et al. 1985) and the $\Delta(B - V)$ between the reddened and comparison stars. The third Fitzpatrick criterion requires a good luminosity and temperature match (i.e. UV spectral type) between the detailed spectra of the reddened and comparison stars. The errors in the the UV spectral types are ~ 1 temperature subclass and ~ 1 luminosity class (Neubig & Bruhweiler 1997).

We applied these criteria to the candidate reddened stars and found only one star, AZV 214,

in addition to the three stars identified in §2, which satisfied all three of the Fitzpatrick criteria. Thus, we are left with a small sample of 4 reddened stars with which we can study the UV extinction in the SMC. Table 2 lists the spectral and photometric data for the four reddened and four comparison stars. The UV spectral types are from Neubig & Bruhweiler (1997). The optical and infrared photometry was taken from Bouchet et al. (1985), except for AZV 70 which was taken from Ardeberg & Maurice (1977). The uncertainties in the optical and infrared photometry are 0.02, 0.045, 0.02, 0.028, 0.032, and 0.027 for V , $(U - V)$, $(B - V)$, $(J - V)$, $(H - V)$, and $(K - V)$, respectively (Ardeberg & Maurice 1977; Bouchet et al. 1985; Bouchet 1997). Table 3 displays the $\Delta(B - V)$, $\Delta(U - B)/\Delta(B - V)$, and ΔV_o values for the reddened and comparison pairs.

3.1. Calculation of Extinction Curves

We calculated extinction curves using the standard pair method (Massa, Savage, & Fitzpatrick 1983) which uses a reddened star and an appropriately chosen unreddened comparison star. The extinction curves were calculated using

$$E(\lambda) = \frac{\Delta(\lambda - V)}{\Delta(B - V)} = \frac{m(\lambda - V)_r - m(\lambda - V)_c}{(B - V)_r - (B - V)_c} \quad (1)$$

where the subscripts r and c refer to the reddened and comparison stars, respectively. Individual short (SWP) and long (LWR and LWP) IUE spectra were coadded resulting in a single spectrum extending from 1300 Å to 3200 Å. The spectra were coadded using the nearest neighbor method with bad points (as defined by the NEWSIPS quality vector) excluded. The individual spectra were weighted by their exposure times. The resulting long and short wavelength spectra were binned to the instrumental resolution of ~ 5 Å. The two spectra were then merged at the maximum wavelength in the short wavelength spectrum. Table 4 tabulates the *IUE* spectra we used.

Uncertainties in the extinction curves were calculated using the method of Massa, Savage, & Fitzpatrick (1983) and Cardelli, Sembach, & Mathis (1992). It is no longer necessary to estimate the uncertainties in the *IUE* fluxes as these are calculated in the NEWSIPS reduction. The uncertainties in the extinction curve were calculated using

$$\sigma[E(\lambda)] = E(\lambda) \sqrt{\left(\frac{\sigma[\Delta(\lambda - V)]}{\Delta(\lambda - V)}\right)^2 + \left(\frac{\sigma[\Delta(B - V)]}{\Delta(B - V)}\right)^2} \quad (2)$$

where

$$\sigma[\Delta(B - V)] = \sqrt{\sigma[(B - V)_r]^2 + \sigma[(B - V)_c]^2}, \quad (3)$$

$$\sigma[\Delta(\lambda - V)] = \sqrt{\sigma[m(\lambda)_r]^2 + \sigma[V_r]^2 + \sigma[m(\lambda)_c]^2 + \sigma[V_c]^2}, \quad (4)$$

$$\sigma[m(\lambda)] = \frac{-2.5}{2} \log \left(\frac{F(\lambda) - \sigma[F(\lambda)]}{F(\lambda) + \sigma[F(\lambda)]} \right), \quad (5)$$

$$\sigma[F(\lambda)] = \sqrt{\sigma[F(\lambda)_{\text{NEWSIPS}}]^2 + [\sigma_{\text{repeat}} F(\lambda)]^2}; \quad (6)$$

Table 2. Stellar Data

type ^a	AZV	SK	UV sp. type	Optical sp. type	ref ^b	V	(U-V)	(B-V)	(J-V)	(H-V)	(K-V)
r	18	13	B3 Ia	B2 Ia	L97	12.40	-0.75	0.01	-0.03	-0.05	-0.08
c	462	145	B2 Ia	B1.5 Ia	L97	12.54	-1.04	-0.14	0.35	0.40	0.41
r	214		B2 Ia	B3 Iab	G87	13.35	-0.72	0.05	0.02	0.00	-0.03
c	380	120	B1 1a:	B0.5:	B85	13.50	-1.00	-0.11	0.27	0.29	0.37
r	398		O9 Ia:	O9.7 Ia	B85	13.86	-0.70	0.08	-0.22	-0.25	-0.26
c	289	103	O9 Ia	B0 I	B85	12.37	-1.09	-0.15	0.24	0.29	0.34
r	456	143	O8 II	O9.7 Ib	B85	12.90	-0.69	0.07	-0.08	-0.10	-0.10
c	70	35	O9 Ia	O9.5 Iw	H83	12.39	-1.13	-0.16

^ar = reddened star, c = comparison star

^bH83 = Humphreys 1983, B85 = Bouchet et al. 1985, G87 = Garmany et al. 1987, L97 = Lennon 1997

Table 3. Fitzpatrick Criteria

reddened	comparison	$\Delta(B - V)$	$\frac{\Delta(U-B)}{\Delta(B-V)}$	ΔV_o
AZV 18	AZV 462	0.15 ± 0.03	0.93 ± 0.42	-0.55 ± 0.09
AZV 214	AZV 380	0.16 ± 0.03	0.75 ± 0.31	0.59 ± 0.09
AZV 398	AZV 289	0.23 ± 0.03	0.70 ± 0.26	0.86 ± 0.10
AZV 456	AZV 70	0.24 ± 0.03	0.75 ± 0.23	-0.13 ± 0.10

$F(\lambda)$ is the *IUE* measured flux; $\sigma[F(\lambda)_{\text{NEWSIPS}}]$ is the uncertainty NEWSIPS calculates; $\sigma_{\text{repeat}} \sim 0.05\%$ is the estimated uncertainty in the relative *IUE* calibration (the difference between two spectra of the same object taken by *IUE* [Garhart & Nichols 1994]). We have not included an error term for temperature or luminosity mismatch as they are not easily quantifiable. Also, Cardelli et al. (1992) have shown that these uncertainties are smaller than those calculated using equation 2. The uncertainties (as calculated in equation 2) in the UV extinction curves can be divided into two parts. One part arises from random uncertainties in the UV data and the magnitude of this uncertainty can be reduced by binning the UV data. The other part arises from random uncertainties in the optical photometry and relative calibration of *IUE* which cannot be reduced by binning the UV data. Thus, a lower limit to the uncertainty in the UV extinction can be calculated by assuming $\sigma[F(\lambda)_{\text{NEWSIPS}}] = 0$ in equation 6. The resulting minimum uncertainties at all UV wavelengths are 22, 19, 13, & 13% for AZV 18, 214, 398, & 456, respectively. This illustrates the drawback of using moderately reddened stars for extinction curve work.

We fit each extinction curve with the Fitzpatrick & Massa (1990, hereafter FM) parameterization of the UV extinction curve. This parameterization has a functional form with 3 terms. The first is a linear term (c_1 [y-intercept] and c_2 [slope]). The second is a Lorentzian-like “Drude” profile for the 2175 Å bump (c_3 [strength], x_o [bump center], and γ [bump width]). The third is a curvature term for the far-UV ($x > 5.9 \mu\text{m}^{-1}$, c_4 [strength]).

3.1.1. AZV 18

The extinction curve for AZV 18 has been determined previously (Prévot et al. 1984; Thompson et al. 1988). The comparison star which best satisfies the Fitzpatrick criteria is AZV 462. This star was one of the three comparison stars used in Prévot et al. (1984). We only used the extinction curve from the comparison star with the best spectral match. Averaging extinction curves made with multiple comparison stars degrades the final extinction curve since the most accurate extinction curve has then been averaged with less accurate extinction curves. Figure 1a displays the spectra of AZV 18 and AZV 462. The extinction curve for AZV 18 is shown in Figure 1b. The FM fit parameters are tabulated in Table 5.

3.1.2. AZV 214

The UV extinction curve for the star AZV 214 has never been calculated previously. This is likely due to the presence of another early-type star only 7''5 away. Both stars were included within the *IUE* observing aperture. In order to separate the spectrum of AZV 214 from the nearby star, we used the MGEX and NEWCALIB routines provided in the IUEIDL package to extract and calibrate the spectrum for AZV 214 and the nearby star. Neubig & Bruhweiler (1997)

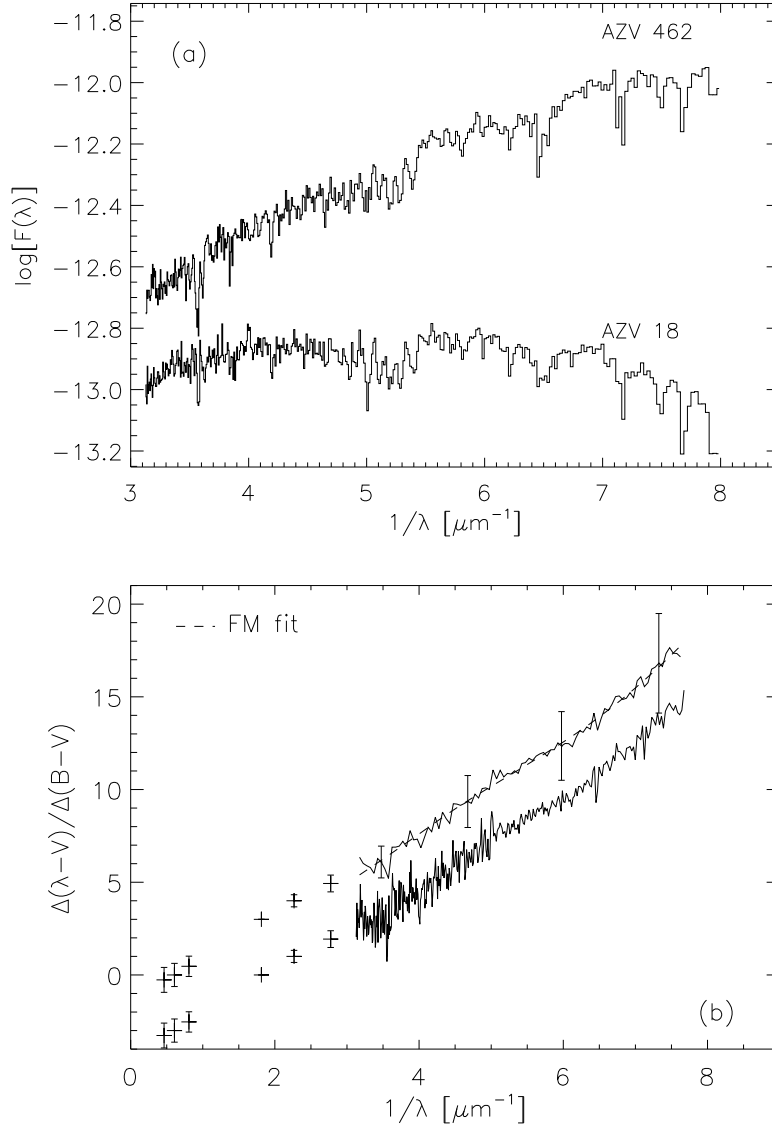


Fig. 1.— The spectrum of reddened star AZV 18 and its comparison star AZV 462 are plotted in (a). The extinction curve derived for AZV 18 is displayed in (b) without any binning (lower) and with bins of $0.05 \mu\text{m}^{-1}$ and shifted by $\Delta E(\lambda) = 3$ (upper). Plot (b) also shows the FM fit for this extinction curve.

determined the UV spectral type using the combined spectrum of the two stars. This resulted in a UV spectral type too late for AZV 214 since the nearby star had the effect of decreasing the intensity of the spectral lines. The optical and infrared photometry of AZV 214 are likely unaffected by the nearby star as the flux from this star, relative to AZV 214, is already small at 3000 Å and decreasing to the red. The nearby star is bluer than AZV 214 and is probably an unreddened O type star.

The comparison star which best satisfies the Fitzpatrick criteria is AZV 380. Figure 2a displays the spectra of AZV 214 and AZV 380. The extinction curve for AZV 214 is shown in Figure 2b. The FM fit parameters are tabulated in Table 5.

3.1.3. AZV 398

The extinction curve for AZV 398 has been determined previously (Prévot et al. 1984; Rodrigues et al. 1997). The comparison star which best satisfies the Fitzpatrick criteria is AZV 289. This star was one of the eight comparison stars used in Prévot et al. (1984) and one of the five stars used in Rodrigues et al. (1997). Again, by using only the comparison star with the best spectral match we were able to determine a more accurate extinction curve. Figure 3a displays the spectra of AZV 398 and AZV 289. The extinction curve for AZV 398 is shown in Figure 3b. The FM fit parameters are tabulated in Table 5.

3.1.4. AZV 456

The star AZV 456 is the only star in the SMC to show the signature of the 2175 Å extinction bump in its spectrum (Figure 4a). We have chosen a different comparison star than previous authors (Lequeux et al. 1982; Rodrigues et al. 1997) specifically to remove mismatches in the C IV and Si IV lines which are sensitive to both luminosity and temperature (Neubig & Bruhweiler 1997). Figure 4a displays the spectra of AZV 456 and AZV 70. The extinction curve for AZV 456 is shown in Figure 4b. The FM fit parameters are tabulated in Table 5.

4. Discussion

Any discussion of the behavior of the dust in the SMC based on only four extinction curves is obviously severely hampered by the small sample size. Yet, interesting trends can be seen even in this small sample. The four extinction curves are plotted together in Figure 5 and their FM fit parameters are tabulated in Table 5. The extinction curves for AZV 18, 214, & 398 are very similar and are all roughly linear with λ^{-1} . The extinction curve for AZV 456 is much different as it has a significant 2175 Å bump and a weaker far-UV extinction. The similarity of the extinction

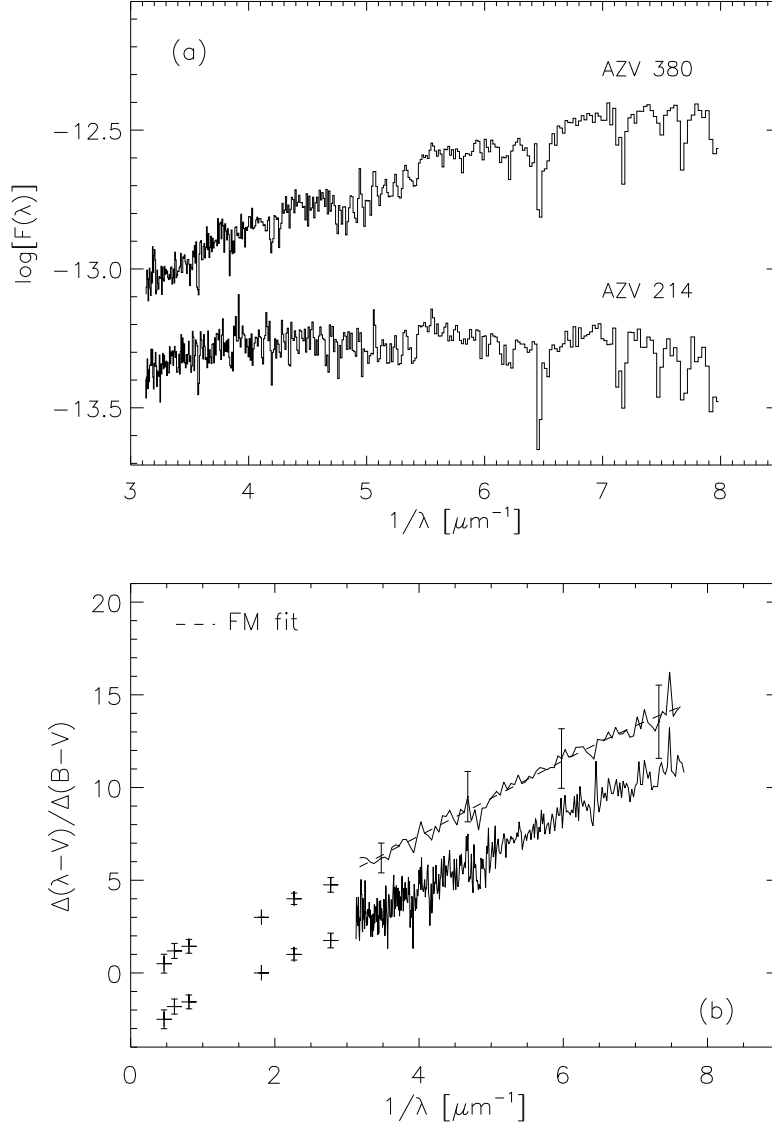


Fig. 2.— The spectrum of reddened star AZV 214 and its comparison star AZV 380 are plotted in (a). The extinction curve derived for AZV 214 is displayed in (b) without any binning (lower) and with bins of $0.05 \mu\text{m}^{-1}$ and shifted by $\Delta E(\lambda) = 3$ (upper). Plot (b) also shows the FM fit for this extinction curve.

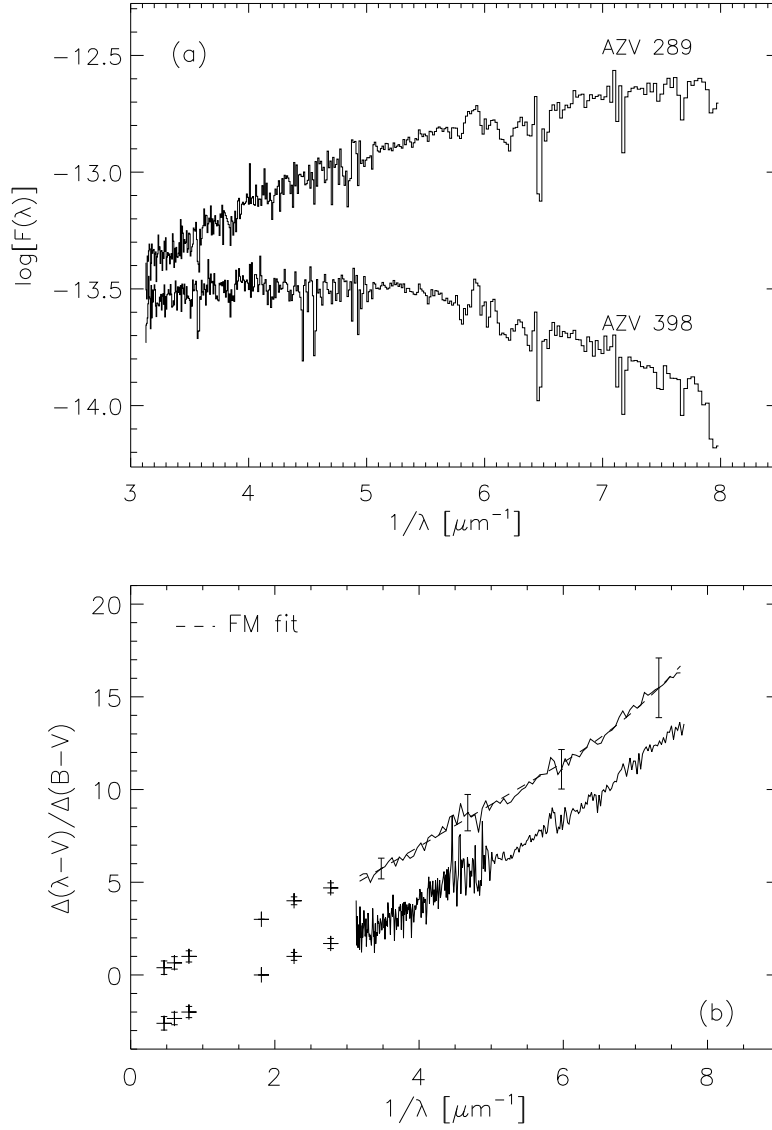


Fig. 3.— The spectrum of reddened star AZV 398 and its comparison star AZV 289 are plotted in (a). The extinction curve derived for AZV 398 is displayed in (b) without any binning (lower) and with bins of $0.05 \mu\text{m}^{-1}$ and shifted by $\Delta E(\lambda) = 3$ (upper). Plot (b) also shows the FM fit for this extinction curve.

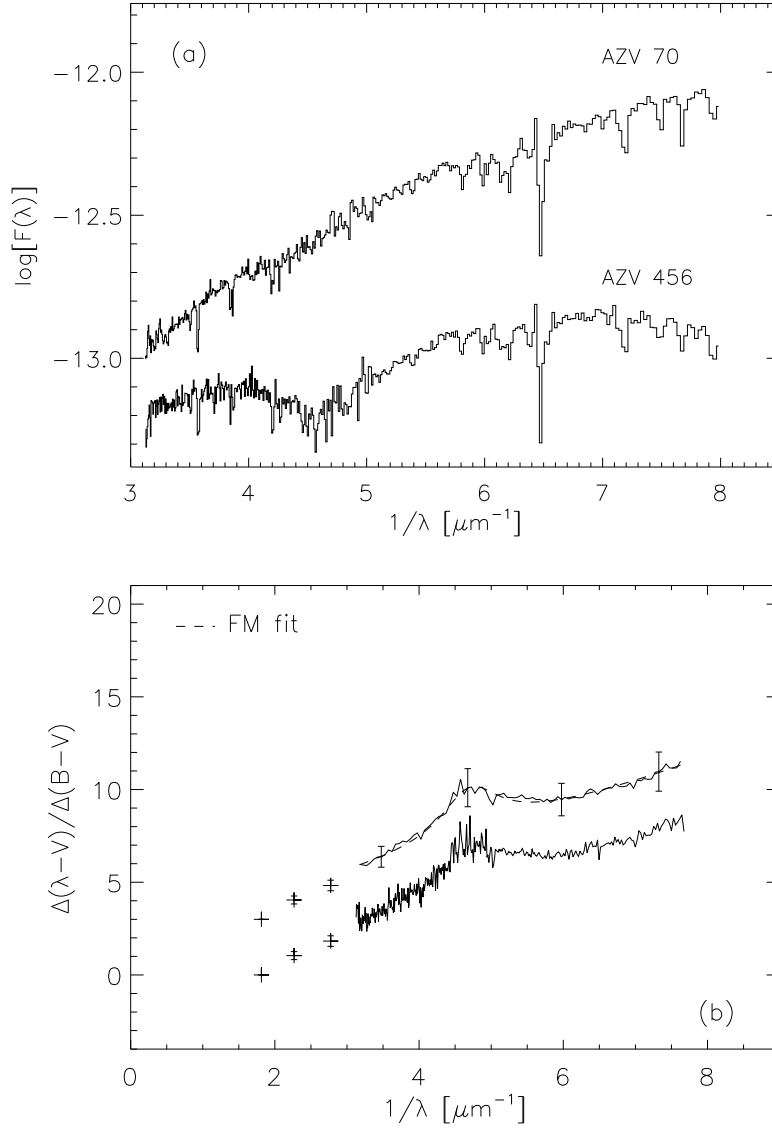


Fig. 4.— The spectrum of reddened star AZV 456 and its comparison star AZV 70 are plotted in (a). The extinction curve derived for AZV 456 is displayed in (b) without any binning (lower) and with bins of $0.05 \mu\text{m}^{-1}$ and shifted by $\Delta E(\lambda) = 3$ (upper). Plot (b) also shows the FM fit for this extinction curve.

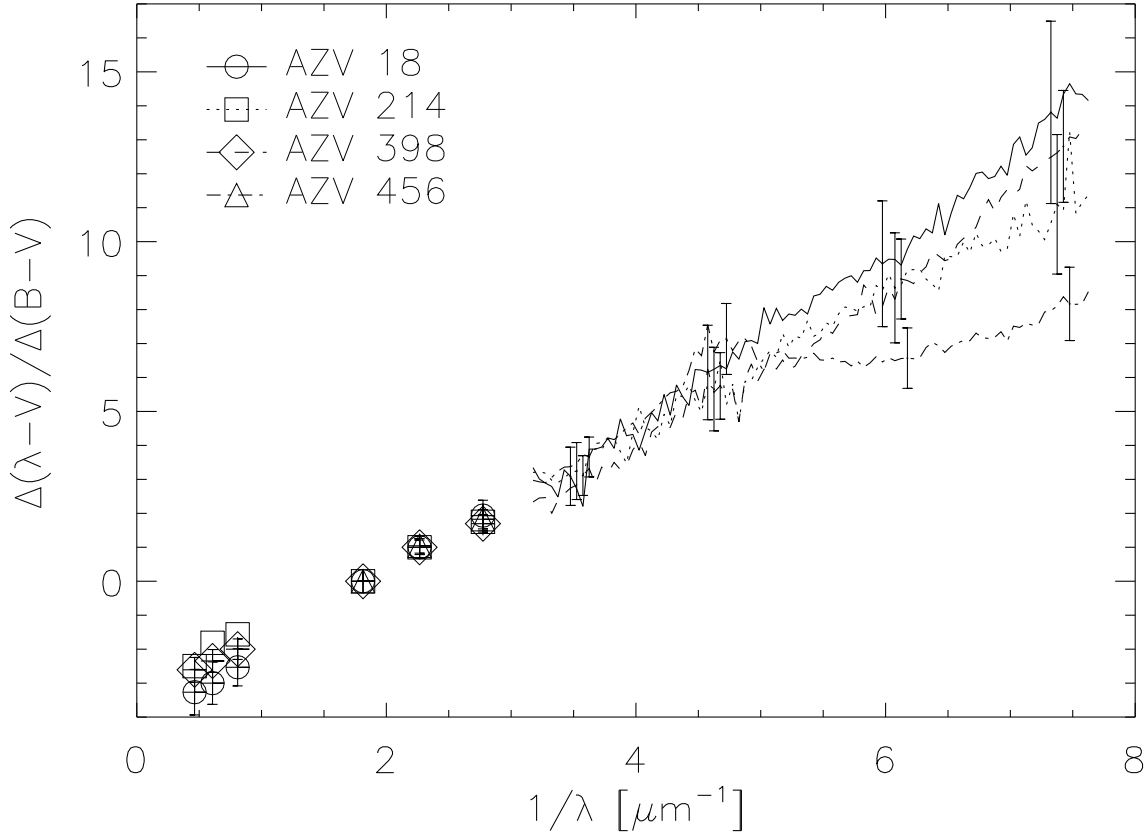


Fig. 5.— The four extinction curves for AZV 18, 214, 398, & 456 are plotted.

curves for AZV 18 & 214 (lightly reddened) to that of AZV 398 (more reddened) gives confidence that the extinction curves for AZV 18 & 214 are real.

Since the extinction curve for AZV 456 looks more like Milky Way dust than SMC dust, one wonders if a large fraction of this extinction is due to foreground Galactic dust. Velocity resolved H I measurements toward AZV 456 show that 90% of the H I along the line-of-sight is located in the SMC (Lequeux et al. 1982; McGee & Newton 1981, 1982). Also, the star AZV 454, which is 1.5 from AZV 456, shows very little evidence of reddening. These observations strongly imply that most of the interstellar medium along the line of sight toward AZV 456 lies in the SMC.

In the Milky Way, most of the differences between extinction curves can be explained by the variation in the single parameter $R_V = A(V)/E(B - V)$. This parameter measures the average dust grain size with R_V increasing with increasing average grain size (CCM). Following Bouchet

Table 4. *IUE* Data

AZV	<i>IUE</i> Spectra
18	SWP 8295/10321/18014/18015 LWR 7241/14207
70	SWP 16621/18830–LWP 12387
214	SWP 22372–LWR 17263
289	SWP 16049–LWR 12345
380	SWP 10319–LWR17265
398	SWP 18911/22361–LWR 14963
456	SWP 16051/45199 LWR 12347–LWP 23556
462	SWP 10316–LWR 17259

Table 5. FM fit parameters

AZV	c_1	c_2	c_3	x_o	γ	c_4
18	-5.68 ± 0.28	2.53 ± 0.05	0.76 ± 1.38	4.56 ± 0.23	1.68 ± 1.52	0.60 ± 0.26
214	-3.72 ± 0.29	2.03 ± 0.05	0.09 ± 3.03	4.98 ± 1.97	5.12 ± 19.24	-0.20 ± 0.26
398	-5.16 ± 0.29	2.27 ± 0.05	0.14 ± 11.29	4.41 ± 17.06	-6.48 ± 211.22	0.80 ± 0.28
456	-0.96 ± 0.09	1.18 ± 0.02	2.57 ± 0.22	4.71 ± 0.01	1.00 ± 0.05	0.10 ± 0.15

et al. (1985), the R_V values for the four SMC extinction curves were calculated from

$$R_V = 1.10 \frac{\Delta(V - K)}{\Delta(B - V)}. \quad (7)$$

The intrinsic colors of the reddened stars were assumed to be either the colors of their respective comparison stars or the intrinsic colors of Galactic stars of the same spectral types as tabulated in Johnson (1966) for $(B - V)$, and Koornneef (1983), for $(V - K)$. The values of R_V calculated both ways are tabulated in Table 6. The two R_V values are equivalent within the uncertainties and the adopted values are contained in the last column of Table 6. The four extinction curves have roughly similar values of R_V . If the SMC dust followed a CCM-like relationship then AZV 456 would have the largest R_V . This does not seem to be the case.

In order to investigate the dependence of the extinction in the SMC on environment, we plotted the positions of the four stars on an $H\alpha$ image of the SMC (Figure 6). The $H\alpha$ intensities trace star formation activity. The lines-of-sight toward all four stars are associated with the known H II regions (Davies, Elliott, & Meaburn 1976; Caplan et al. 1996). The three stars with roughly linear extinction curves (AZV 18, 214, & 398) are located in regions of high $H\alpha$ intensities (SMC Bar). The one star (AZV 456) with a more Galactic type extinction curve is also located in an H II region but one with much weaker star formation (SMC Wing). The H II region associated with the line-of-sight to AZV 214 is noteworthy because it is associated with the cluster NGC 346 which is the most massive star formation region in the SMC. NGC 346 contains 33 known O type stars (Massey, Parker, & Garmany 1989). The $H\alpha$ flux from this cluster is 10% of that seen from 30 Dor in the LMC (Massey, Parker, & Garmany 1989). The $H\alpha$ fluxes from the H II regions along the lines-of-sight toward AZV 18, 398, & 456 are 1, 1, and 0.1%, respectively, of that seen for 30 Dor (Kennicutt & Hodge 1986; Caplan et al. 1996). The dust along the AZV 456 sightline has likely been exposed to a less harsh environment than the other three sightlines.

It is known that processing of Galactic dust near regions of active star formation results in changes in the UV extinction curve (Mathis & Cardelli 1992). A similar behavior is seen in the 30 Dor region in the LMC (Fitzpatrick 1986). It is clear from this work that the harsh radiation and

Table 6. R_V Values

star	comparison	Galactic	adopted
AZV 18	3.60 ± 0.73	2.78 ± 0.34	3.60 ± 0.73
AZV 214	2.75 ± 0.55	2.36 ± 0.21	2.75 ± 0.55
AZV 398	2.87 ± 0.40	3.05 ± 0.17	2.87 ± 0.40
AZV 456	...	2.66 ± 0.16	2.66 ± 0.16

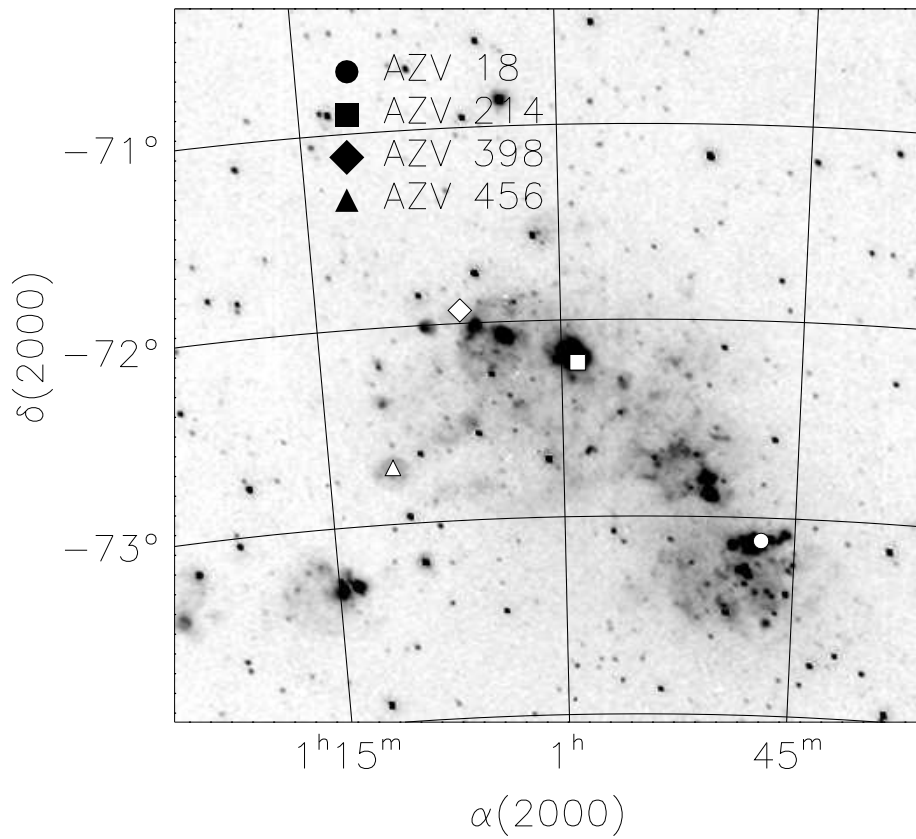


Fig. 6.— The positions of the four reddened stars are plotted on a $H\alpha$ image of the SMC (Bothun 1997). This image is displayed in the North Celestial Pole projection (Staveley-Smith et al. 1997). The image was provided by G. Bothun and L. Staveley-Smith.

shock environment associated with star formation regions is modifying the dust in the SMC. In all three galaxies, star formation modifies nearby dust by altering the 2175 Å bump and increasing the strength of the far-UV extinction. Yet, the extent of the modification does *not* seem to be well correlated with the level of star formation activity. Figure 7 plots the average extinction curves for the LMC (30 Dor and rest of LMC, [Fitzpatrick 1986]), the SMC (Bar and Wing), and the Milky Way ($R_V = 3.1$). The extinction curve for θ^1 Ori D, a star in the Orion H II region, is also plotted. The average extinction curve for the SMC Bar is similar to the previous SMC average extinction curve (Prévot et al. 1984). From this figure, it is obvious that the extinction in the SMC Bar is unlike that which has been found anywhere except starburst galaxies (Gordon et al. 1997). On the other hand, the extinction in the SMC Wing is similar to that found in the LMC (excluding the 30 Dor region) and the Milky Way open cluster Trumpler 37 (not shown, Clayton & Fitzpatrick 1987; FM). The large difference between the extinction curve in the Orion H II region and the SMC Bar implies that an Orion-like H II region is not enough to produce starburst-like dust. Something more is needed.

This raises the question: Why are the extinction properties of the dust in the SMC Bar so much more extreme than that found in the 30 Dor region of the LMC? The largest star formation region in the SMC (NGC 346) has only 10% the activity of 30 Dor as measured by $H\alpha$ (Caplan et al. 1996). The extinction curve for AZV 456 shows that dust, very similar to Galactic and LMC dust, exists in the SMC. Therefore, there must be some significant environmental difference between the LMC 30 Dor and SMC Bar regions which affects the extent to which star formation activity can modify dust. One known difference between the LMC and SMC is metallicity. The metallicities of the LMC and SMC are 0.2 and 0.6 dex lower, respectively, than the that of the local Galactic ISM (the ISM is 0.1 dex lower than solar). However, the relative abundances of the elements in the LMC and SMC are similar to that found in the local interstellar medium (Russell & Dopita 1992). Metallicity is correlated with the dust-to-gas ratio in galaxies (Issa, MacLaren, & Wolfendale 1990). So, the amount of dust in the SMC is significantly lower than that found in the LMC. This could affect the ability of dust grains in the SMC to shield themselves from the radiation and shocks present near star formation regions. This contrasts with the finding that starburst galaxies all possess dust with an extinction curve like that found in the SMC Bar even though they have metallicities between 0.1 and 2.0 solar (Gordon et al. 1997). It is possible that the much higher level of star formation present in starburst galaxies ($10\times$ that of 30 Dor) overwhelms other environmental factors and always produces SMC Bar-like dust. The starburst galaxies were UV selected biasing the sample toward intrinsically bright, nearby starbursts with at least one lightly reddened starburst region. Thus, the combination of a small column of dust and the more intense star formation possibly accounts for the presence of SMC-like dust in all starburst galaxies studied in Gordon et al. (1997).

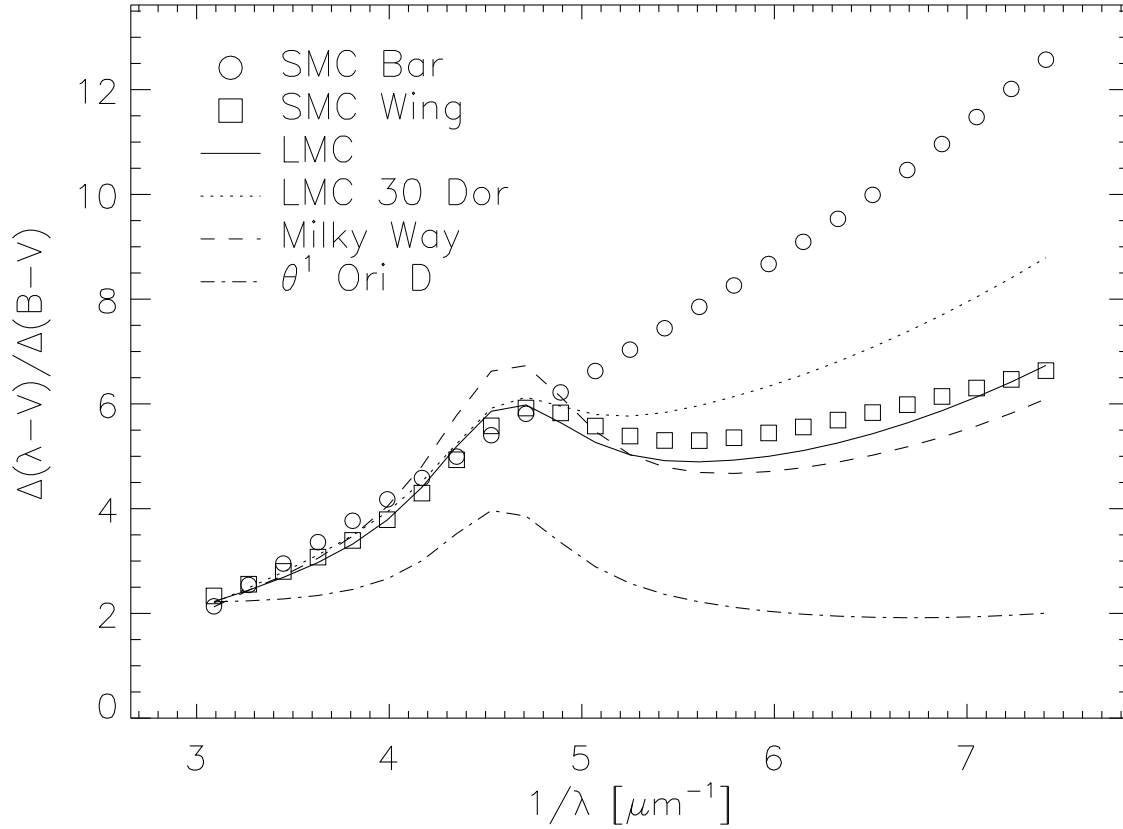


Fig. 7.— The extinction curves for the SMC, LMC, and Milky Way are plotted. The curves plotted are those calculated from the FM fits except for the Milky Way which was calculated from the CCM relationship for an $R_V = 3.1$. The extinction curve for the SMC Bar is the $\Delta(B - V)$ weighted average of the curves for AZV 18, 214, & 398. The SMC Wing and θ^1 Ori D extinction curves have been multiplied by 0.83 and 1.3, respectively, to allow easier comparison to the other four curves.

5. Summary

- We have greatly improved the UV extinction curves for the SMC through improvements in the S/N of the IUE spectra and careful choices of reddened and comparison star pairs.

- Four reddened SMC stars possess the Fitzpatrick criteria needed for accurate extinction calculations. Three of the four stars possess a roughly linear (with λ^{-1}) extinction curve. The lines-of-sight toward these three stars (AZV 18, 214, & 398) pass through active star formation regions. The fourth star (AZV 456) has an extinction curve with a 2175 Å bump and a weaker far-UV rise. Its sightline also passes through a star formation region, but one which is much less active.

- Processing of dust near regions of star formation results in variations in UV extinction. However, there is no simple correlation between the strength of the variations and the amount of star formation activity. Other parameters such as galaxy metallicity must also play an important role.

- As this work is based on only four sightlines, more observations of reddened stars in the SMC are needed for to confirm these results. Of special need are observations outside the SMC Bar to confirm the extinction curve of AZV 456.

We thank G. Bothun and L. Staveley-Smith for giving us the H α image. This work was supported by NASA grant NAG5-3531.

REFERENCES

- Ardeberg, A. & Maurice, E. 1977, A&AS, 30, 261
- Azzopardi, M. & Vigneau, J. 1979, A&AS, 35, 353
- Azzopardi, M. & Vigneau, J. 1982, A&AS, 50, 291
- Azzopardi, M., Vigneau, J., & Macquet, M. 1975, A&AS, 22, 285
- Bianchi, L., Clayton, G. C., Bohlin, R. C., Hutchings, J. B., & Massey, P. 1996, ApJ, 471, 203
- Bothun, G. 1997, private communication
- Bouchet, P., Lequeux, J., Maurice, E., Prévot, L., & Prévot-Burnichon, M. L. 1985, A&A, 149, 330
- Bouchet, P. 1997, private communication
- Bromage, G. E. & Nandy, K. 1983, MNRAS, 204, 29P

- Calzetti, D., Kinney, A. L., & Storchi-Bergmann, T. 1994, *ApJ*, 429, 582
- Caplan, J., Ye, T., Deharveng, L., Turtle, A. J., & Kennicutt, R. C. 1996, *A&A*, 307, 403
- Cardelli, J. A., Clayton, G. C., & Mathis, J. S. 1989, *ApJ*, 345, 245 (CCM)
- Cardelli, J. A., Sembach, K. R., & Mathis, J. S. 1992, *AJ*, 104, 1916
- Clayton, G. C. & Fitzpatrick, E. L. 1987, *AJ*, 92, 157
- Clayton, G. C., et al. 1996, *ApJ*, 460, 313
- Clayton, G. C. & Martin, P. G. 1985, *ApJ*, 288, 558
- Davies, R. D., Elliott, K. H., & Meaburn, J. 1976, *MmRAS*, 81, 89
- Franx, M., Illingworth, G. D., Kelson, D. D., van Dokkum, P. G., & Tran, K.-V. 1997, *ApJ*, 486, L75
- Fitzpatrick, E. L. 1985, *ApJ*, 299, 219
- Fitzpatrick, E. L. 1986, *AJ*, 92, 1068
- Fitzpatrick, E. L. & Massa, D. 1990, *ApJS*, 72, 163 (FM)
- Garhart, M. P. & Nichols, J. S. 1994, in *IUE Newsletter* No. 55, 1
- Garmany, C. D., Conti, P. S., & Massey, P. 1987, *AJ*, 93, 1070
- Gordon, K. D., Calzetti, D., & Witt, A. N. 1997, *ApJ*, in press (1 Oct)
- Humphreys, R. 1983, *ApJ*, 265, 176
- Issa, M. R., MacLaren, I., & Wolfendale, A. W. 1990, *A&A*, 236, 237
- Johnson, H. L. 1966, *ARA&A*, 4, 193
- Kennicutt, R. C., Jr. & Hodge, P. W. 1986, 306, 130
- Kinney, A. L., Bohlin, R. C., Calzetti, D., Panagia, N., & Wyse, R. F. G. 1993, *ApJS*, 86, 5
- Koornneef, J. 1983, *A&A*, 128, 84
- Lennon, D. J. 1997, *A&A*, 317, 871
- Lequeux, J., Maurice, E., Prévot-Burnichon, M.-L., Prévot, L., Rocca-Volmerange, B. 1982, *A&A*, 113, L15
- Lequeux, J., Maurice, E., Prévot, L., Prévot-Burnichon, M.-L., Rocca-Volmerange, B. 1984, in *Structure and Evolution of the Magellanic Clouds*, IAU Symp. 108, eds. S. van den Bergh & K. S. de Boer (Dordrecht: Reidel) 405

- Lowenthal, J. D., et al. 1997, *ApJ*, 481, 673
- Madau, P., Pozzetti, L., & Dickinson, M. 1997, *ApJ*, in press
- Massa, D., Savage, B. D., & Fitzpatrick, E. L. 1983, *ApJ*, 266, 662
- Massey, P., Lang, C. C., DeGioia-Eastwood, K., & Garmany, C. D. 1995, *ApJ*, 438, 188
- Massey, P., Parker, J. W., & Garmany, C. D. 1989, *AJ*, 98, 1305
- Mathis, J. S. & Cardelli, J. A. 1992, *ApJ*, 398, 610
- McGee, R. X. & Newton, L. M. 1981, *Proc. Astro. Soc. of Australia*, 4, 189
- McGee, R. X. & Newton, L. M. 1982, *Proc. Astro. Soc. of Australia*, 4, 308
- Nandy, K., McLachlan, A., Thompson, G. I., Morgan, D. H., Willis, A. J., Wilson, R.,
Gondhalekar, P. M., & Houziaux, L. 1982, *MNRAS*, 201, 1P
- Neubig, M. M. S. & Bruhweiler, F. C. 1997, *AJ*, in press
- Nichols, J. S., Garhart, M. P., De La Peña, M. D., & Levay, K. L. 1994, *New Spectral Image
Processing System Information Manual: Low Dispersion Data - Version 1.0, IUE Newsletter
No. 53*
- Pettini, M., Steidel, C. C., Adelberger, K. L., Kellogg, M., Dickinson, M., Giavalisco, M. 1997, in
ORIGINS, ASP Conference Series, eds. J. M. Shull, C. E. Woodward, & H. Thronson, in
press (astro-ph/9708117)
- Prévot, M. L., Lequeux, J., Maurice, E., Prévot, L., Rocca-Volmerange, B. 1984, *A&A*, 132, 389
- Rocca-Volmerange, B., Prévot, L., Ferlet, R., Lequeux, J., & Prévot-Burnichon, M. L. 1981, *A&A*,
99, L5
- Rodrigues, C. V., Magalhães, A. M., Coyne, G. V., & Piirola, V. 1997, *ApJ*, 485, 618
- Russell, S. C. & Dopita, M. A. 1992, *ApJ*, 384, 508
- Sanduleak, N. 1968, *AJ*, 73, 246
- Sanduleak, N. 1969, *AJ*, 74, 877
- Staveley-Smith, L., Sault, R. J., Hatzidimitriou, D., Kesteven, M. J., & McConnell, D. 1997,
MNRAS, 289, 225
- Steidel, C. C., Giavalisco, M., Pettini, M., Dickinson, M., & Adelberger, K. L. 1996, *ApJ*, L17
- Thompson, G. I., Nandy, K., Morgan, D. H., & Houziaux, L. 1988, *MNRAS*, 230, 429

Trager, S. C., Faber, S. M., Dressler, A., & Oemler, A., Jr. 1997, *ApJ*, 485, 92

Walborn, N. R. 1991, in *Massive Stars in Starbursts*, eds. C. Leitherer et al. (Cambridge: Cambridge Univ. Press), 145